STRUCTURAL OPTIMIZATION INCORPORATING CENTRIFUGAL AND CORIOLIS EFFECTS

89-1310-CP

Howard D. Gans*
Department of Aeronautics and Astronautics
Air Force Institute of Technology
Wright-Patterson AFB OH 45433

William J. Anderson**
Department of Aerospace Engineering
The University of Michigan
Ann Arbor MI 48109

Abstract

The problem of structural optimization in the presence of centrifugal and Coriolis effects was studied for a rotating blade and for a rotating beam. A finite element formulation was used and optimization was performed by applying nonlinear inverse perturbation. Centrifugal forces were modeled by the use of differential stiffness in a small displacement approximation, and Coriolis effects were obtained by employing Coriolis finite element matrices. The nonlinear inverse perturbation scheme was then modified to account for the mild geometric nonlinearities posed by differential stiffness and was also modified to incorporate the complex phase changes resulting from Coriolis effects. Finally, the method was applied to small and large changes in the fundamental (bending) frequency of two rotating systems. Satisfactory results were obtained.

Nomenclature

A_e	Element Planform Area
$[b_e]$	Element Coriolis matrix
d	Desired value (super- or subscript)
e	Elemental subscript
[H]	General system matrix
[K]	System stiffness matrix
$[K_o]$	Infinitesimal displacement stiffness matrix
$[\bar{k}_e]$	Cubic expansion element stiffness
[M]	System mass matrix
M_i	Generalized Mass for ith mode
m	Element mass
p, c	Predictor, corrector (super- or subscript)
[N']	First derivative, shape function matrix
{q}	Displacement vector
r_0	Radial distance to element centroid
t_e	element thickness
α_e	Element change property
Δ	Perturbation operator
$[\phi]$	Matrix of eigenvectors
$\{\phi\}$	Real eigenvector
$\{\psi\}$	Complex eigenvector
$\{\xi\}$	Imaginary eigenvector
ω	Eigenfrequency
$[\omega]$	Diagonal matrix of eigenfrequencies
Ω	Rotational speed (hz)
% Δ	Percent desired frequency change
% ΔW	Percent weight change
$(\dot{})$	Time derivitive

Introduction

The techniques of structural optimization can be applied to the original design of a component or can be used to perform structural redesign. Some structures, because of their application, are subject to body forces in addition to the loadings caused by boundary forces. Rotating bodies experience centrifugal and Coriolis effects. In the rotating frame, the centrifugal effects may be viewed as a reversed-effective pseudo-force. If the rotational speed is small enough, these forces can be neglected. In high-speed applications, however, the body forces must be taken into account.

Centrifugal force in particular can result in stiffening. The rotating blades in a high-speed compressor and turbine are subject to these body forces. With the advent of higher-speed blading, it is necessary to include thiseffect in design. This introduces a nonlinearity in the finite element analysis and optimization scheme.

*Assisstant Professor, Aerospace Engineering
Member AIAA

**Professor, Aerospace Engineering
Member AIAA

Coriolis force is another body "force" that a rotating body may experience when viewed in a rotating coordinate system. This force, also known as gyroscopic force, couples motion in one plane with motion in another plane. Gyroscopic effects are velocity dependent; that is, the greater the velocity in one plane, the greater the effect will be in the other plane. In systems which permit large amounts of out-of-plane motion, such as in pretwisted blades, the Coriolis forces will become great at high speeds, and thus will affect optimal redesign.

Literature Survey

If a baseline structure exists but it is found that the response of the structure is unacceptable and modification is necessary, perturbation techniques may be employed to obtain the desired values. Stetson[1] introduced small changes in mass and in stiffness moduli of a structure. He used a first order perturbation method that obtained the mode shapes for the perturbed structure. He introduced the concept of "admixture coefficients" that expressed the mode shapes of the perturbed structure in terms of combinations of the baseline mode shapes. Stetson and Harrison[2] expanded this technique to encompass a finite element structural formulation and applied it to several problems. Sandström and Anderson[3] related Stetson's admixture coefficients to physical changes in the finite element model. Kim et al[4] obtained a complete nonlinear inverse perturbation technique using the equations of dynamic equilibrium. A SUMT penalty function method was used where objective function was minimum weight and the penalty term involved a normalized set of residual force vectors.

One major problem of the nonlinear inverse perturbation method is that for a large problem, the number of calculations required become excessive. For that reason, Kim and Anderson[5] used generalized dynamic reduction to transform the problem into a small sized subspace. Hoff et al[6] overcame the difficulties in applying the nonlinear inverse perturbation method by using an incremental predictor-corrector technique. In the predictor phase, element changes necessary to enforce the desired mode shape and frequency changes are obtained through a first order solution of the dynamic equations. In the corrector, approximate eigenvectors are obtained for the objective system, which are then used to correct the elemental changes.

Queau and Trompette[7] applied changes in inertia properties during the redesign process to determine changes in centrifugal stiffening affecting optimization. Their method also involved linear design sensitivites. It also did not update the eigenvectors during the optimization process, requiring a large number of calculations. Only beam elements were used, and their procedure cannot be used on a general class of problems, particularly plate-like bodies.

Theoretical Formulation

Equation of Motion

The equation of motion for an unforced conservative system including Coriolis but no damping may be written as:

$$[M]\{\ddot{q}\} + [B]\{q\} + [K]\{q\} = \{0\} \tag{1}$$

To describe a rotating system in the presence of centrifugal effects, the total stiffness matrix $[K_{TOT}]$ may be expressed by:

$$[K_{TOT}] = [K_0] + [K_D] \tag{2}$$

$[K_D]$ is the differential stiffness matrix for the assembled system, often called geometric stiffness or initial stress matrix, and models the mild structural nonlinearity due to applied loads. Centrifugal effects may be considered just such an applied load, and the element differential stiffness matrix, may be expressed by:[8]

$$[k_D^e] = \int_V [N']^T \begin{bmatrix} [s] & [0] & [0] \\ [0] & [s] & [0] \\ [0] & [0] & [s] \end{bmatrix} [N'] \, dV \tag{4}$$

where $[s]$ is the matrix of applied stresses such that:

$$[s] = \begin{bmatrix} \sigma_{x0} & \tau_{xy0} & \tau_{xz0} \\ \tau_{xy0} & \sigma_{y0} & \tau_{yz0} \\ \tau_{xz0} & \tau_{yz0} & \sigma_{zo} \end{bmatrix} \tag{5}$$

The matrix [B] represents the assembled, skew-symmetric, system Coriolis matrix. The derivation of the element Coriolis matrix is fully described by Gans[9].

Eigenvalue Problem for Conservative Coriolis Systems

Equation (1) represents the problem in free vibration of a conservative Coriolis system. The solution to this equation is of the form:

$$\{q(t)\} = e^{pt}\{q\} \tag{6}$$

where p is a constant complex scalar and $\{q\}$ is a constant complex vector. Equation (6) is introduced into Equation (1) and the following characteristic equation is obtained:

$$\left|p^2[M] + p[B] + [K]\right| = 0 \tag{7}$$

This equation gives a polynomial of degree 2n in p. Due to the symmetry of the mass and stiffness matrices and the skew symmetry of the Coriolis matrix, all of the odd powers of p are absent from the characteristic equation. The eigenvalues will consist of n pure imaginary conjugate pairs, $p_r = \pm i\omega_r$, where $r = 1,2,\ldots n$. The eigenvectors will also occur in complex conjugate pairs, $\{q\}_r = \{y\}_r + i\{z\}_r$, $\{\bar{q}\}_r = \{y\}_r - i\{z\}_r$, where $\{y\}_r$ is the real part and $i\{z\}_r$ is the imaginary part of the eigenvector $\{q\}_r$. This implies that the amplitude ratios will not, in general, be real. Therefore, the components of an eigenvector pair for a given

eigenvalue pair will oscillate at the same frequency but not in phase.

Perturbation Methods Including Differential Stiffness

We first wish to determine the influence of element thickness upon the differential stiffness matrix of beam and plate elements. Let Ω be the rotational frequency of a structure about an axis perpendicular to its rotation. The centrifugal force F applied to an element of the structure with centroid at a radial distance r_0 from the axis of rotation, and mass m. is given by:

$$F = 4\pi^2\Omega^2 r_0 m \tag{8}$$

This illustrates that the centrifugal force is linearly dependent on thickness. In Equation (4), the differential stiffness matrix is linearly dependent on the centrifugal force, though the constant of proportionality may be dependent on geometry. Therefore, we can say:

$$[k_D^e] \propto t \tag{9}$$

This implies that a change in thickness will effect the element differential stiffness matrix linearly.

Stetson and Palma[10] related baseline and objective systems through perturbations of the baseline system quantities. The stiffness and mass matrices are perturbed by:

$$[k'] = [k] + [\Delta k] \tag{10}$$

and

$$[m'] = [m] + [\Delta m] \tag{11}$$

These perturbations will cause perturbations in the dynamic response. The perturbations in the eigenvalue and eigenvector matrices are given by:

$$[\omega'^2] = [\omega^2] + [\Delta(\omega^2)] \tag{12}$$

$$[\phi'] = [\phi] + [\Delta\phi] \tag{13}$$

The structural changes described in Equations (10) and (11) can be decomposed into p element change properties where a group of elements may be allowed to change. Thus

$$[\Delta k] = \sum_{e=1}^{p} [\Delta k_e] \tag{14}$$

$$[\Delta m] = \sum_{e=1}^{p} [\Delta m_e] \tag{15}$$

Furthermore, each element change can be expressed as a fractional change α_e from the baseline system. The change α_e may represent a change in element thickness. In general, α_e can be expressed by:

$$[\Delta k_e] = [k_e]\alpha_e \tag{15}$$

$$[\Delta m_e] = [m_e]\alpha_e \tag{16}$$

For plates, the bending component of the stiffness matrix, owever,varies as the cube of the plate thickness. Therefore, Equation (16) is replaced by:

$$[\Delta k_e] = [k_{e_{memb}}]\alpha_e + [k_{e_{diff}}]\alpha_e + [k_{e_{bend}}](3\alpha_e + 3\alpha_e^2 + \alpha_e^3) \tag{17}$$

where $[k_{e_{memb}}]$ contains the membrane components, $[k_{e_{diff}}]$ contains the differential stiffness components, and $[k_{e_{bend}}]$ contains the bending components of $[k_e]$.

Equation (18) also holds for beams, with the exception that the element stiffness matrix containing only extensional properties, $[k_{e_{ext}}]$, replaces $[k_{e_{memb}}]$.

Steston developed a matrix eigenvalue and eigenvector redesign method using perturbation. The generalized form without Coriolis terms is given by:

$$\{\psi'\}_j^T [\Delta k]\{\psi'\}_i - \omega_i'^2 \{\psi'\}_j^T [\Delta m]\{\psi'\}_i = \{\psi'\}_j^T [m]\{\psi'\}_i \omega_i'^2 - \{\psi'\}_j^T [k]\{\psi'\}_i \tag{19}$$

for i,j = 1,2,...,n.

For the case of non-repeated eigenvalues, Sandström and Anderson[11] obtained the following expression, nonlinear in the element change property α_e, for the physical mode shape change for the kth degree of freedom:

$$\Delta\psi_{ki} = \sum_{e=1}^{p} \left\{ \sum_{j=1}^{n} \left[\frac{\psi_{kj}}{M_j(\omega_i^2 - \omega_j^2)} \left\{ \{\psi\}_j^T ([k_{e_{memb}}] + [k_{e_{diff}}])\{\psi\}_i + \alpha_e \{\psi\}_j^T [k_{e_{bend}}]\{\psi\}_i (3\alpha_e + 3\alpha_e^2 + \alpha_e^3) - \omega_i^2 \{\psi\}_j^T [m_e]\{\psi\}_i \alpha_e \right\} \right] \right\} \quad (\text{for } j \neq i) \tag{20}$$

Similarly, using the relationship for the change in the element mass matrix, Equation (17), and the nonlinear relationship for the change in the element stiffness matrix, Equation (18), results in the following expression, nonlinear in the element change property α_e, that describes the change in the natural frequency to the ith mode:

$$\Delta(\omega_i^2) = M_i^{-1} \sum_{e=1}^{p} \left[\{\psi\}_i^T ([k_{e_{memb}}] + [k_{e_{diff}}])\{\psi\}_i \alpha_e + \{\psi\}_i^T [k_{e_{bend}}]\{\psi\}_i (3\alpha_e + 3\alpha_e^2 + \alpha_e^3) - \omega_i^2 \{\psi\}_i^T [m_e]\{\psi\}_i \alpha_e \right] \tag{21}$$

In applying the method described above in finite element analysis, practical considerations make it necessary to divide the quadrilateral elements in the finite element model into two elements: one with only membrane stiffness and one with only out-of-plane (flexural) stiffness. These elements are then superimposed. This permits multiplication of the stiffness terms representing membrane properties by a linear element change factor while the stiffness terms containing the flexural properties can be altered by a nonlinear change factor.

Perturbations of the System Including Coriolis Effects

When the original system is modified in the optimization process, it can be said to be perturbed. The perturbed system must also obey the equations of equilibrium. Let the perturbed system be distinguished from the original by primes. Therefore, the equations of motion for the perturbed system in free vibrations including Coriolis effects may be written as:

$$[M']\{\ddot{\phi}'\}_i + [B']\{\dot{\phi}'\}_i + [K']\{\phi'\}_i = \{0\} \tag{22}$$

A solution is now assumed:

$$\{\phi'\}_i = \{\psi'\}_i e^{i\omega'_i t} \tag{23}$$

This results in the following equation for the perturbed system:

$$-[\psi']^T[M'][\psi'][\omega'^2]+i[\psi']^T[B'][\psi'][\omega'] +[\psi']^T[K'][\psi'] = 0 \tag{24}$$

The perturbed system can be related to the original, unprimed system by:

$$[H'] = [H] + [\Delta H] \tag{25}$$

The global changes in mass and stiffness in terms of element change properties have been defined previously. Similarly, the global change in the Coriolis matrix is given by:

$$[\Delta B] = \sum_{e=1}^{p} [\Delta b_e] \tag{26}$$

and

$$[\Delta b_e] = [b_e]\alpha_e \tag{27}$$

The last equation is justified because, as we have seen, the Coriolis matrix is linearly dependent on element mass. The element mass is itself linearly dependent on changes in thickness; the element change parameter.

Equations (26), (27), and the relationsips for mass and stiffness perturbations are applied to (24). Terms in Δ of order 2 or higher are eliminated as are the baseline equilibrium terms. The equations are expanded for all modes and an expression for the change in the eigenvalue in terms of admixture coefficients, c_{ij}, is obtained, such that:

$$[\Delta\phi] = [\phi][c]^T \tag{28}$$

where c_{ij} are small and $c_{ii} = 0$. This results in the following expression for the change in natural frequency in scalar form:

$$\begin{aligned}&\{\psi\}_j^T [\Delta K]\{\psi\}_i + i\omega_i \{\psi\}_j^T [\Delta B]\{\psi\}_i - \omega_j^2 \{\psi\}_j^T [\Delta M]\{\psi\}_i \\ &= \{\psi\}_i^T [M]\{\psi\}_i \Delta(\omega_i^2) - i\{\psi\}_i^T [B]\{\psi\}_i \Delta\omega \qquad (i=j) \\ &= (\{\psi\}_j^T [M]\{\psi\}_i (\omega_j^2 - \omega_i^2) - i\{\psi\}_j^T [B]\{\psi\}_i (\Delta\omega_j - \Delta\omega_i))c_{ij} \\ &(i\neq j)\end{aligned} \tag{29}$$

Applying the definitions for the changes in the structural matrices to the above equation and setting i=j, one obtains the following expression for the frequency change for the ith mode due to application of the element changes α_e:

$$\begin{aligned}&\{\psi\}_i^T [M]\{\psi\}_i \Delta(\omega_j^2) - i\{\psi\}_i^T [B]\{\psi\}_i \Delta\omega_i \\ &= \sum_{e=1}^{p} (\{\psi\}_i^T [\tilde{k}_e]\{\psi\}_i + i\omega_i \{\psi\}_i^T [b_e]\{\psi\}_i \\ &\quad - \omega_i^2 \{\psi\}_i^T [m_e]\{\psi\}_i)\alpha_e\end{aligned} \tag{30}$$

where

$$[\tilde{k}_e] = [k_{e_{memb}}] + [k_{e_{diff}}] + 3[k_{e_{bend}}] \tag{31}$$

However, it must be remembered that the eigenvector itself is a complex quantity with both amplitude and phase components. Let us express the complex eigenvector for the ith mode $\{\psi\}$ as:

$$\{\psi\}_i = \{\phi\}_i + i\{\xi\}_i \tag{32}$$

Therefore, Equation (30) becomes two equations; one that equates real parts and another one that equates imaginary parts. These are, respectively,

$$\begin{aligned}&(\{\phi\}_i^T [M]\{\phi\}_i - \{\xi\}_i^T [M]\{\xi\}_i)\Delta(\omega_i^2) \\ &+ \{\xi\}_i^T [B]\{\xi\}_i \Delta(\omega_i) \\ &= \sum_{e=1}^{p} \left\{ \{\phi\}_i^T [\tilde{k}_e]\{\phi\}_i - \{\xi\}_i^T [\tilde{k}_e]\{\xi\}_i \right. \\ &\quad \left. - \left(\{\phi\}_i^T [m_e]\{\phi\}_i - \{\xi\}_i^T [m_e]\{\xi\}_i \right) \omega_i^2 \right\} \alpha_e\end{aligned} \tag{33}$$

and

$$2\{\phi\}_i^T [M]\{\xi\}_i \Delta(\omega_i^2) - (\{\phi\}_i^T [B]\{\phi\}_i \quad (34)$$

$$+ \{\xi\}_i^T [B]\{\xi\}_i)\Delta\omega_i$$

$$= \sum_{e=1}^{p} \left\{ 2\{\phi\}_i^T [\tilde{k}_e]\{\xi\}_i \right.$$

$$+ \left(\{\phi\}_i^T [b_e]\{\phi\}_i + \{\xi\}_i^T [b_e]\{\xi\}_i \right) \omega_i$$

$$\left. - 2\{\phi\}_i^T [m_e]\{\xi\}_i \omega_i^2 \right\} \alpha_e$$

Note that for the case of no Coriolis terms and purely real eigenvectors, Equation (33) degenerates to Equation (21) and Equation (34) becomes identically satisfied.

To determine the eigenvector change in the Coriolis system, the admixture coefficients c_{ij} previously defined in Equation (28) can be used. From these admixture coefficents, the eigenvectors of the perturbed system can be obtained:

$$\Delta\psi_{ki} = \sum_{e=1}^{p} \left\{ \sum_{j=1}^{n} \left[\frac{\psi_{kj}}{\{\psi\}_i^T [M]\{\psi\}_i(\omega_i^2 - \omega_j^2) - i\{\psi\}_i^T [B]\{\psi\}_i(\omega_i - \omega_j)} \right.\right.$$

$$\left.\left. \times \left\{ \{\psi\}_j^T [\tilde{k}_e]\{\psi\}_i \alpha_e + i\omega_i \{\psi\}_j^T [b_e]\{\psi\}_i \alpha_e - \omega_i^2 \{\psi\}_j^T [m_e]\{\psi\}_i \alpha_e \right\} \right] \right\}$$

(for $j \neq i$) (35)

Optimal Redesign Methodology

The predictor-corrector method for optimal redesign is developed by first defining the element change property α_e by:

$$\alpha_e = \frac{\Delta t_e}{t_e} \quad (36)$$

The first design change seeks a 10% increase in the fundamental flexural modal frequency. In the predictor step, we will assume that the element change α_e is small; therefore, the quantity $(1+\alpha_e)^3 - 1$ may be approximated by $3\alpha_e$. This results in a 3.11% error, but is done so as to facilitate solving for α_e, which we shall see will be the unknown in the inverse perturbation scheme.

The predictor relates the change in the element change properties to a prescribed change in the desired eigenfrequency. In this way the equation predicts what the system configuration should be for a given amount of frequency change. In the absence of Coriolis effects, Equation (21) serves as the predictor equation. For the complex case involving Coriolis effects, Equations (33) and (34) act as the predictor equations. Note that in that case there are two predictor equations.

For a single element case, the predictor can be solved as one equation with one unknown. For multiple elements, the excess unknown element change properties can be found by optimizing some function, such as minimum weight or minimum structural change. The predictor then becomes an equality constraint in the optimization scheme. In the Coriolis problem, there are two equality constraints. Therefore, it is seen that the problem becomes one of parametric optimization, with thickness as the parameter to be optimizaed.

In the examples below, the augmented Lagrange multiplier method is used to solve the problem in optimization using the Automated Design Synthesis (ADS) program.[12] In addition to the equality constraint or constraints provided by the predictor equations, inequality constraints are also formulated. The first inequality constraint requires α_e to be greater than -0.5. This ensures that the element thickness will always be positive during the redesign process and in no case will an element be reduced by more than 50%. This makes certain that unwanted secondary effects, such as static failure due to the "applied" centrifugal load will not occur. The second inequality constraint forces the α_e to be less than 1E5. This supplies an upper bound to the search procedure. The function to be minimized in the first example is the design change:

$$f(\{\alpha_e\}) = \sum_{e=1}^{p} (\alpha_e)^2 \quad (37)$$

Alternatively, the function to be minimized could be minimum weight. For a system of uniform density, this function is given by:

$$f(\{\alpha_e\}) = \sum_{e=1}^{p} A_e \alpha_e \quad (38)$$

The element change properties determined from Equations (37) or (38) are used to recompute the cross sectional area and moments of intertia for each element. A reanalysis is then accomplished to determine the eigenvalues and eigenvectors. The perturbed eigenvectors are necessary to perform the corrector.

The corrector examines the potential energy imbalance between the system output from the predictor and the desired system and corrects the imbalance through additional element changes. This enforces the natural frequency constraint on the ith mode. The following equation represents that energy balance for the example with no Coriolis effects and is used as the corrector equation:

$$\sum_{e=1}^{p} (\{\psi'\}_i^T [\tilde{k}_e]\{\psi'\}_i - \omega'^2_i \{\psi'\}_i^T [m_e]\{\psi'\})\alpha_e \quad (39)$$

$$= \omega'^2_i \{\psi'\}_i^T [M]\{\psi'\}_i - \{\psi'\}_i^T [K]\{\psi'\}_i$$

If Coriolis effects are included, then two equations, representing the energy balance equation, the first equating real parts and the second equating imaginary parts, are used for the corrector:

$$\sum_{e=1}^{p}\Big[\Big[\{\phi'\}_i^T[\tilde{k}_e]\{\phi'\}_i - \{\xi'\}_i^T[\tilde{k}_e]\{\xi'\}_i \qquad (40)$$

$$- \Big(\{\phi'\}_i^T[m_e]\{\phi'\}_i - \{\xi'\}_i^T[m_e]\{\xi'\}_i\Big)\omega'^2_i\Big]\alpha_e$$

$$= (\{\phi'\}_i^T[M]\{\phi'\}_i - \{\xi'\}_i^T[M]\{\xi'\}_i)\omega'^2_i$$

$$- (\{\phi'\}_i^T[K]\{\phi'\}_i - \{\xi'\}_i^T[K]\{\xi'\}_i)$$

and

$$\sum_{e=1}^{p}\Big[2\{\phi'\}_i^T[\tilde{k}_e]\{\xi'\}_i + \Big(\{\phi'\}_i^T[b_e]\{\phi'\}_i \qquad (41)$$

$$+ \{\xi'\}_i^T[b_e]\{\xi'\}_i\Big)\omega'_i - 2\{\phi'\}_i^T[m_e]\{\xi'\}_i\omega'^2_i\Big]\alpha_e$$

$$= 2\{\phi'\}_i^T[M]\{\xi'\}_i\omega'^2_i - (\{\phi'\}_i^T[B]\{\phi'\}_i$$

$$+ \{\xi'\}_i^T[B]\{\xi'\}_i)\omega'_i - 2\{\phi'\}_i^T[K]\{\xi'\}_i$$

Notice that when the Coriolis effects are absent, the above equations degenerate to those used previously.

The perturbed eigenvectors may be obtained in one of two ways. The first method, mentioned above, is to simply run the predictor system. This yields the full, nonlinearly-perturbed matrix of eigenvectors and the desired mode can be easily partioned out. The second procedure involves the applications of Equation (20) in the absence of Coriolis effects or Equation (35) if Coriolis effects are present. These equations are linear approximations of the perturbations in the eigenvectors. However, using the results of reanalysis, one obtains the full, nonlinear changes in the eigenvector.

Optimal Redesign Examples

Rotating Compressor Blade

The first example problem is a curved rotating blade, of which the finite element model is shown in Figure 1. The blade is made of Inconel 718 steel, has a radius of 254.0 mm, and rotates at a speed of 200 hz. It has an angle of attack of 30 degrees and is modeled after a NACA 64 airfoil. This is a blade typically found in a jet engine high-pressure compressor.

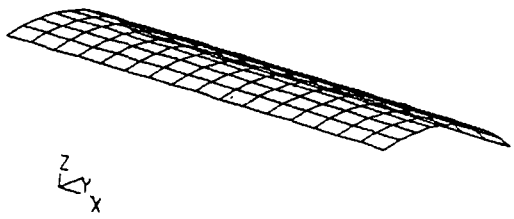

Figure 1. Rotating Blade

The finite elements are each divided into two subelements; one with membrane properties only and another superimposed element with only bending properties. This particular finite element model has approximately 1000 degrees of freedom. The elements are grouped (linked) into twelve regions (Figure 2). During the analysis, the thickness of the regions will change, but the elements within each region will maintain a common thickness. (Each superimposed membrane and bending element will also keep a common thickness.) Regions 1 through 3 have thickness 1.734 mm, Regions 4 through 6 have thickness 2.312 mm, Regions 7 through 9 have thickness 3.005 mm, and regions 10 through 12 have thickness 3.467 mm. This represents an airfoil that is 5% thick at the tip and 10% thick at the root.

10	7	4	1
11	8	5	2
12	9	6	3

Figure 2. Blade Regions

For the nonrotating system, the fundamental frequency is 7.6656E3 rad/sed. For the rotating system including centrifugal effects, the fundamental frequency is 8.3802E3 rad/sec. This implies a 9.32% increase in fundamental frequency due to the centrifugal effect of rotation. Figure 3 shows the first mode shape for the rotating blade, including centrifugal effects.

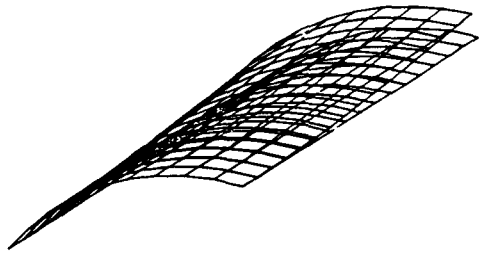

Figure 3. Mode Shape 1, Blade Rotational Effects Included

The problem of the rotating blade was analyzed for several cases and using several different methods to account for nonlinearities. In cases 1 and 2, a 10% increase in the fundamental eigenfrequency was desired, with the objective function for case 1 being minimum change and the objective function for case 2 being minimum weight. Centrifugal effects were included in both the structural analysis and the optimization, but Coriolis effects were neglected. Results of both predictor and corrector are shown in Table 1. Tthe predictor results can be considered to be results from a linear, one-step analysis since the effect of redesign on the eigenvectors does not enter into the predictor procedure. Improvements from the predictor to corrector step show the benefit of the use of nonlinear optimization techniques.

In Table 1, the first column denotes the objective functions used in the predictor and the corrector, respectively. The symbol C/C denotes minimum change in both steps. If W/W is indicated, minimum weight was used in both the predictor and corrector. The use of W/C which, symbolizes that mimimum weight was used in the predictor while minimum change was used in the corrector, indicates a hybrid approach which shall be described later.

Figure 4 shows the final spanwise optimized thickness of the structure for Case 1. Figure 5 shows the final optimized shape of the structure for Case 2. Notice that in the minimum change example, emphasis is given to adding material at the root. In the minimum weight-minimum weight example (Case 2), all of the regions except for the root have been reduced to the lower limit on thickness. This is the pathological case in optimization where the system is driven to an extreme. When this is done in this example, undesirable side effects occure, such as mode switching. The first bending mode is no longer the fundamental frequency and the solution to the problem in optimization is no longer dependable. The frequency results shown for the corrector are for the bending mode; however, this frequency is technically no longer ω_1. A way out of this quandary can be found by a close examination of the results of the predictor. This step obtains 99% of the desired frequency change and also a weight reduction of 14%. Therefore, this solution is close to the frequency constraint, and only a small change is necessary to satisfy it. This implies that a hybrid approach involving a predictor step with a minimum *weight* objective function and a corrector with a minimum *change* objective function could work.

The results of this hybrid approach are shown in Case 3 and Figure 6. In this example, material is added at the root but proportionally less than in the minimum change-minimum change situation. Emphasis is given to removing material from the outboard regions, with most material removed form the second set of elements from the end. Since minimum weight is the objective of the predictor, it is not suprising that more material is removed in Case 3 than in the Case 1 situation.

Two other problems were studied; both involved large (30%) changes in the fundamental frequency. In Case 4, the 30% change is accomplished in one step. A second iteration is performed to obtain an improved solution (Case 5). In another situation, the 30% change is broken down into three 10% increments (Cases 6 through 8). In both of these examples, only a minimum change optimization function is used. Table 2 shows the results of the iterative procedure. The linear predictor step obtains the desired frequency change with less than 24% accuracy, but at the end of the first iteration, the desired frequency change is accomplished to within less than 1%. The second iteration is done for completeness and gives the desired change in fundamental frequency to within 1/100 of 1%.

In Table 3, each increment obtains the desired change in frequency for that increment. The final increment, which completes the 30% change, gives the desired change to within 9/100 of 1%. These two Tables show that excellent accuracy on the frequency goal is obtained, showing the feasibility of making large changes.

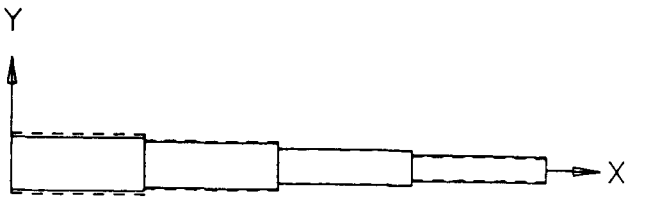

Figure 4. Optimally Redesigned Blade, Case 1 Minimum Change

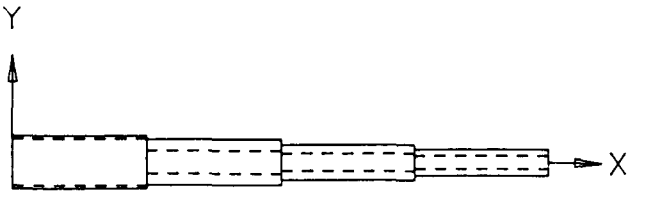

Figure 5. Optimally Redesigned Blade, Case 2 Minimum Weight

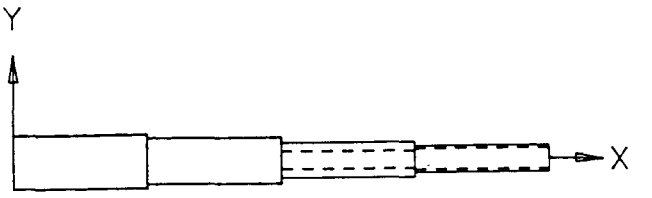

Figure 6. Optimally Redesigned Blade, Case 3 Hybrid

In the optimization procedure, the optimizer itself is run iteratively, with the solution of the previous step becoming the starting point for the succeeding step (the initial starting point is the origin). In nonlinear mathematical programming, the approach is to minimize the objective function while driving the equality constraint function to zero. In no case were more than seven optimizer runs required.

Rotating Beam Incorporating Coriolis Effects

The next example will consider the case of a rotating cantilever beam. The beam itself is aluminum 2024T-6 of length L equal to 250 mm, with moment of inertia I equal to 3.2552E4 mm^4, cross-sectional area A of 625 mm^2, Young's modulus E of 73.77E3 MPa, Poisson's ratio ν equal to 0.33, and density ρ of 2.774E-9 Mg/mm^3. The beam rotates at a speed of 300 hz.

For the nonrotating problem, the frequency for the first mode, which is a bending mode, is 2.093729E3 rad/sec. When centrifugal effects are included in addition, the fundamental frequency is 2.952001E3 rad/sec, an increase of 40.99%. When Coriolis effects are included in addition, the fundamental frequency drops slightly to 2.951942E3 rad/sec. The inclusion of Coriolis forces in the rotating problem decreases the fundamental frequency by -2.00E-3% from the rotating problem that includes centrifugal but not Coriolis effects.

Table 4 summarizes the results from the optimal redesign of the rotating beam. The notation is the same as for the rotating blade. In Case 9, centrifugal effects are included in both the structural analysis and in the optimization. A minimum *change* objective was used. Case 10 was identical to Case 9; however, the *hybrid* procedure was utilized (incorporating a minimum *weight* objectivefunction in the predictor and a minimum *change* objective function in the corrector). Coriolis effects were included in Case 11 in both the structural analysis and equations of constraint. Optimization was accomplished using a minimum *change* objective function.

Table 1. Optimization Results for Blade, 10% Change

Case	Opt.	ω_1(E3)	ω_1^d(E3)	ω_1^p(E3)	$\%\Delta_p$	$\%\Delta W_p$	ω_1^c(E3)	$\%\Delta_c$	$\%\Delta W_c$
1	C/C	8.380	9.218	9.246	103.	4.09	9.220	100.	.025
2	W/W	8.380	9.218	9.210	99.1	-14.1	8.948	67.7	-37.3
3	W/C	8.380	9.218	9.210	99.1	-14.1	9.217	99.9	-14.0

Table 2. Optimization Results for Blade, 30% Change

Iterative Procedure, Minimum Change

Case	Opt.	ω_1(E3)	ω_1^d(E3)	ω_1^p(E3)	$\%\Delta_p$	$\%\Delta W_p$	ω_1^c(E3)	$\%\Delta_c$	$\%\Delta W_c$
4	C/C	8.380	10.89	11.47	123.	13.7	10.92	101.	9.80
5	W/W	10.02	10.89	10.89	100.	9.68	10.89	100.	9.68

Table 3. Optimization Results for Blade, 30% Change

Incremental Procedure, Minimum Change

Case	Opt.	ω_1(E3)	ω_1^d(E3)	ω_1^p(E3)	$\%\Delta_p$	$\%\Delta W_p$	ω_1^c(E3)	$\%\Delta_c$	$\%\Delta W_c$
6	C/C	8.380	9.218	9.246	103.	4.09	9.220	100.	.025
7	C/C	9.220	10.06	10.08	103.	8.62	10.07	100.	8.46
8	C/C	10.07	10.90	10.91	102.	13.7	10.90	100.	13.6

Table 4. Optimization Results for Beam, 10% Change, Coriolis Effects Included

Case	Opt.	ω_1(E3)	ω_1^d(E3)	ω_1^p(E3)	$\%\Delta_p$	$\%\Delta W_p$	ω_1^c(E3)	$\%\Delta_c$	$\%\Delta W_c$
9	C/C	2.952	3.247	3.202	84.6	2.01	3.236	96.2	1.86
10	W/C	2.952	3.247	3.142	64.5	-16.1	3.231	94.5	-15.1
11	C/C	2.952	3.247	3.235	95.9	2.63	3.246	99.5	2.68

Summary of Results

The predictor-corrector method breaks the solution of the problem of nonlinear optimal redesign into two parts. The first part, the predictor, solves for the required structural changes for a given required change of frequency. In this step, the effect of structural changes on the mode shapes is not considered. Therefore, this part of the solution may be considered as a conventional linear structural analysis. In the corrector, the efect of the structural changes on the mode shapes is taken into account and the system is once again modified to obtain an improved solution.

In all of the examples involving the rotating blade, the final result of the predictor-corrector approach obtains the desired frequency change to within one percent. In the *minimum change* cases, the linear predictor overshoots the solution by a few percent. The corrector changes the final solution so that the eigenfrequency is at the desired value. Even for large changes, the predictor-corrector method obtains the desired solution if suitable iteration or incrementing is done.

For the rotating beam with a *minimum weight* objective function, the linear predictor undershoots the desired frequency goal by quite a bit, as much as 35%. The corrector obtains the desired frequency to within one percent.

The rotating beam shows some other interesting results. In Case 9, the desired change is obtained within 4%. In case 10, there is a lot of undershoot by the predictor, but the corrector obtains the desired solution within 6%. When both centrifugal and Coriolis forces are included in Case 11, the best solution is found. The linear approach gives an answer to within 5% and the corrector improves this to within 1%. The method used in Case 11 represents the best theoretical formulation. The equations used represent the full nonlinear structural approach with both centrifugal and Coriolis effects.

Comparison with Other Methods

Queau and Trompette obtained minimum weight designs with constraints on frequency. Their method incorporated the centrifugal effects but not Coriolis. In the method implemented here, when minimum weight is employed, the second station from the free end has the minimum thickness and the end bulges out, though it remains less thick than the original design. This was also obtained by Queau and Trompette.

Olhoff and Parbery[13] examined the optimizationof rotating beams with respect to frequency constraints. However, they employed lumped masses which tend to alter the optimized shape from the purely distributed mass approach . Their final shapes indicated tapering except near the region surrounding a lumped mass where bulging then occured.

Conclusions

The predictor-corrector method for structural optimization using inverse perturbation was extended to incorporate centrifugal and Coriolis effects. Centrifugal forces were treated as a static stiffening preload and the Coriolis terms were formulated into a separate velocity-dependent matrix. With Coriolis effects excluded and a frequency constraint involving a ten percent increase in the fundamental eigenfrequency, the linear predictor obtained the required change within two percent for the blade or five percent for the beam. The nonlinear corrector obtained a final optimized system that met the frequency constraint within one percent. Thus the predictor-corrector method for nonlinear redesign obtained excellent agreement between the desired eigenvalue and the calculated eigenvalue.

When Coriolis effects were included, both the magnitude and phase of the components of the fundamental eigenvector were required to obtain the equations of constraint. This complex eigenvalue analysis was adapted to the nonlinear inverse perturbation predictor-corrector approach. The method was applied to the problem of the rotating beam. Once again, the desired frequency change was obtained to within one percent.

The problem of large frequency change (30%) was tried for the rotating blade incorporating centrifugal effects. Both an iterative and incremental solution were accomplished, and in each case the desired frequency was achieved almost exactly. Thus it is seen that the predictor-corrector method is extraordinarily stable, obtaining even large changes with excellent correlation between the desired change in the eigenvalue and the calculated change resulting from the redesign process.

Use of a minimum weight objective function in both the predictor and corrector steps resulted in a pathological solution with all mass concentrated at one area. To correct this deficiency, a minimum change objective function was used in the corrector step. This hybrid approach combined the desired goal of minimum weight with the stability of the minimum change objective function.

In summary, the predictor-corrector method for optimal redesign as extended in this work obtained the desired frequency changes with excellent accuracy. The methods used were applied to several test problems, one being a curved blade with nearly one thousand degrees of freedom. In each case, the desired frequency change was obtained to within a few percent. Therefore, the approach works and can be applied to frequency control problems in optimal redesign of rotating systems.

References

[1]Stetson, K.A., "Perturbation Method of Structural Design Relevant to Holographic Analysis", AIAA Journal, Vol. 13, No. 4, pp. 457-459.

[2]Stetson, K.A. and Harrison, I.R., "Redesign of Structural Vibration Modes by Finite-Element Inverse Perturbation", Journal of Engineering for Power, April 1981, Vol. 103, pp. 319-325.

[3]Sandström, R.E., and Anderson, W.J., "Modal Perturbation Methods for Marine Structures", Transactions of the Society of Naval Architects and Marine Engineers", Vol. 90, pp. 41-54.

[4]Kim, K., Anderson, W.J., and Sandström, R.E., "Nonlinear Inverse Perturbation Method in Dynamic Analysis", AIAA Journal, Vol. 21, No. 9, pp. 1310-1316.

[5]Kim, K. and Anderson, W.J., "Generalized Dynamic Reduction in Finite Element Dynamic Optimization", AIAA Journal, Vol. 22, No. 11, pp. 1616-182.

[6]Hoff, C.J., Bernitsas, M.M., Sandström, R.E., and Anderson, W.J., "Inverse Perturbation Method for Structural Redesign with Frequency and Mode Shape Constraints", AIAA Journal, Vol. 22, No. 9, pp. 1304-1309.

[7]Queau, J.P., Trompette, P., "Optimal Shape Design of Turbine Blades", ASME Paper 81-DET-128, submitted for presentation at the Design Engineering Technical Conference, September 20-23, 1981, Hartford, Connecticut.

[8]Cook, R., Concepts and Applications of Finite Element Analysis, John Wiley and Sons, New York NY, 1974.

[9]Gans, H.D., "Structural Optimization Including Centrifugal and Coriolis Effects", Ph. D. Thesis, The University of Michigan, Ann Arbor MI, 1988.

[10]Stetson, K.A. and Palma, "Inversion of First-Order Perturbation Theory and Its Application to Structural Design", AIAA Journal, Vol. 14, No. 4, pp. 454-460.

[11]Sandström, R.E. and Anderson, W.J., "Modal Perturbation Methods for Marine Structures", Transactions of the Society of Naval Architects and Marine Engineers", Vol. 90, pp. 41-54.

[12]Vanderplaats, G.N., ADS - A Fortran Program for Automated Design Synthesis (Version 1.10), Engineering Design Optimization Inc., Santa Barbara CA, 1985.

[13]Olhoff, N. and Parbery, R., "Designing Vibrating Beams and Rotating Shafts for Maximum Difference Between Adjacent Natural Frequencies", International Journal of Solids and Structures, Vol. 20, No. 1, pp. 63-75.